Original Article

The Possible Role of Bone Marrow Mesenchymal Stem Cells (BM-MSCs) in Ameliorating the Rotenone-Induced Changes on the Substantia Nigra in the Adult Male Albino Rat: Morphometric, Histological, and Immunohistochemical Study

Mohamed N. Mahmoud, Dorreia A. Mohamed, Esraa K. Mohamed and Reneah R. Bushra

Department of Human Anatomy and Embryology, Faculty of Medicine, Assiut University, Assiut, Egypt

ABSTRACT

Introduction: Loss of dopaminergic neurons of the substantia nigra (SN) results in Parkinson's disease (PD). Rotenone is used as an animal model of PD. BM-MSCs are a promising therapy.

Aim of the Work: The work aimed to evaluate the effects of rotenone on the SN and the role of BM-MSCs in ameliorating these effects.

Material and Methods: A total number of 24 rats were randomly divided into three groups. Group A was subdivided into; group A1 (6 rats) received a subcutaneous injection of 5 ml dimethyl sulfoxide (DMSO) /kg every 2 days for two weeks and group A2 (6 rats) received the same regimen for five weeks. Group B (rotenone-treated group) (6 rats) received a subcutaneous injection of a dose of 1.5 mg rotenone /kg dissolved in 5 ml DMSO/kg, once every 2 days for two weeks. Group C (BM-MSCs-treated group) (6 rats) was injected with rotenone with the same regimen as group B, followed by an intraperitoneal injection of one million heterogenous BM-MSCs diluted with 1 ml of saline and sacrificed 3 weeks later. At the destined time, the rats were sacrificed, and the brains were processed for light and electron microscopic examination and immunohistochemistry.

Results: Group B showed a statistically significant decrease in body weight and an increase in brain weight in comparison to the control group A1, signs of neuronal degeneration, Lewy bodies, destructed neuronal ultrastructure, strong positive GFAP, caspase-3, and ubiquitin immunoreactivity with protein aggregation. Group C showed noticeable morphometric, histological, and immunohistochemical improvement.

Conclusion: The rotenone negatively affects the substantia nigra, and the BM-MSCs could ameliorate these effects.

Received: 06 October 2022, **Accepted:** 01 November 2022

Key Words: Albino rat, BM-MSCs, substantia nigra, rotenone.

Corresponding Author: Reneah R. Bushra, MD, Department of Human Anatomy and Embryology, Faculty of Medicine, Assiut University, Assiut, Egypt, **Tel.**: +20 12 0794 9154, **E-mail:** reneah@aun.edu.eg

ISSN: 1110-0559, Vol. 47, No. 1

INTRODUCTION

Substantia nigra (SN) is a critical brain region for dopamine production. SN can be functionally and morphologically divided into two regions, the substantia nigra pars compacta (SNpc) containing dopaminergic neurons and the substantia nigra pars reticulata (SNpr) with inhibitor gamma-aminobutyric acid-containing neurons[1].

Parkinson's disease (PD) is the second most common neurodegenerative disorder. Environmental factors such as exposure to metals, solvents and pesticides or any head injuries lead to the disease. Patients with PD suffer from motor deficits such as tremors, muscle rigidity, bradykinesia, unstable gait, and posture that severely affect patient quality of life[2]. PD results from the progressive loss of the dopaminergic neurons in the nigrostriatal pathway and the formation of intraneuronal inclusions in remaining neurons, namely Lewy bodies and this is a defining pathological characteristic of PD. Current treatments for PD primarily include pharmacological therapies that aim to increase dopamine levels by providing a dopamine precursor. These treatments are effective early alleviating symptoms but are inefficient in ceasing its progression[1].

Various neurotoxin-based models of PD exhibiting noticeable degeneration of nigrostriatal dopaminergic neurons have been developed, such as 6-hydroxydopamine, 1-methyl-4-phenyl-1,2,3,6-tetrahydropyridine, paraquat and rotenone. Rotenone is a natural compound extracted from certain plant roots mainly used to kill vegetable and agricultural pests. It causes a marked decrease in motor coordination activity of experimental rodents in the form of bradykinesia, postural instability, and rigidity. It has gained some reliability as a pesticide model of PD due to its ability to cause selective degeneration of dopaminergic neurons in the nigrostriatum. Being highly hydrophobic, rotenone can cross the blood-brain barrier and inhibit the activity of mitochondria, leading to the production of reactive oxygen species (ROS), and mitochondrial dysfunction[1].

 DOI: 10.21608/ejh.2022.167234.1786

Mesenchymal stem cells (MSCs) are multipotent progenitor cells that can differentiate into a variety of cell types of all three germ layers[3]. Recently, the transplantation of human stem cells has been documented to achieve positive effects in some neurological disease models[4]. Based on the regenerative capacity of stem cells, transplantation therapies of various stem cells have been tested in basic research and preclinical trials, and some have shown great prospects[5]. The ability of the stem cells to differentiate toward any somatic cell type allows the generation of neural cells instead of those implicated in the pathogenesis of neurological diseases[5]. Autologous BM-MSCs treatments of neurodegenerative diseases including PD have manifested tremendous therapeutic efficacy in both disease models and clinical trials[5,6].

AIM OF THE WORK

Hence, the present work aimed to assess the effects of rotenone on the SN and the role of the bone marrow mesenchymal stem cells against these effects.

MATERIAL AND METHODS

Chemicals

Rotenone (CAS no.: 83-79-4) was purchased in white powder form imported from Sigma-Aldrich, St. Louis, MO, USA, by the El-Gomhouria Company for Trading Chemicals and Medical Appliances. Rotenone was dissolved in the vehicle dimethyl sulfoxide (DMSO).

Animals

A total of 24 adult male Wistar albino rats, aged 2 months and weighing 200-250 gm, were obtained from Animal House, Faculty of Medicine, Assiut University. The rats were housed under hygienic measures in metal cages. Food and water were available ad libitum[7].

Isolation and expansion of heterogeneous BM-MSCs

Isolation of heterogeneous BM-MSCs was done at the Tissue Culture and Molecular Biology Centre, Assiut University. BM-MSCs were isolated and expanded from the femurs and tibiae of healthy male albino rats. The animals were anaesthetized, and then the skin was sterilized with 70% ethyl alcohol before cutting the skin. The bones were carefully dissected from adherent soft tissues. Then, they were placed into a sterilized beaker containing 70% ethyl alcohol for 1-2 min. The bones were placed in a Petri dish of phosphate buffer saline for washing and then taken to a laminar airflow cabinet. The ends of the bones were removed using sterile scissors. Bone marrow was collected by rapid infusion of the femurs and tibiae with Dulbecco's modified Eagles medium supplemented with 10% foetal bovine serum and 1% antibiotic (penicillin-streptomycin). To isolate the nucleated cells, density gradient ficoll/paqu was used[8]. After centrifugation, the cells were re-suspended with a serum-supplemented medium and incubated in a 50 cm2 culture flask. The isolated cells were cultured in 20 ml of complete media and incubated at 37°C in a 5% humidified CO2 incubator for 7-10 days as primary culture until the formation of large colonies. The culture was washed with phosphate-buffered saline and released with 0.25% trypsin in 1mm EDTA (5 min at 37°C). On the 10th day of the BM-MSCs culture and by using the inverted microscope, colonies of spindle-shaped stem cells were identified and photographed (Figure 1).

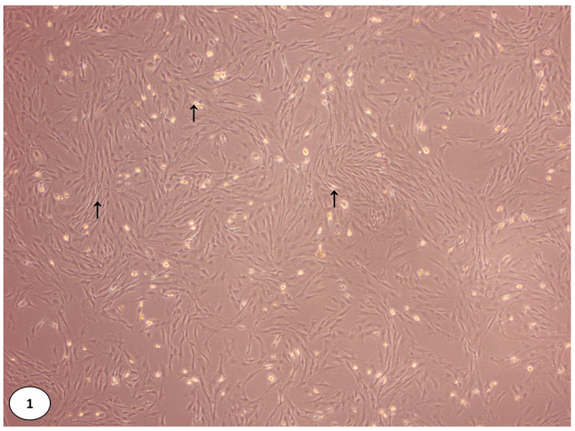

Fig. 1: A photomicrograph of BM-MSCs' culture on the 10th day showing colonies of spindle-shaped stem cells (↑). (X40)

Experimental design

Twenty-four adult male Wistar albino rats were weighed and randomly divided into three groups A, B and C:

Group A (control group): consisted of 12 rats and was divided into group A1 and group A2. Group A1 (6 rats): received a subcutaneous injection of DMSO in a volume of 5ml/kg body weight (b.w.) once every 2 days for 2 weeks[9,10]. At the end of the experiment, the body and brain weights of that group were compared with group B. Group A2 (6 rats): received the same regimen for 5 weeks. At the end of the experiment, the body and brain weights of that group were compared with group C.

Group B (rotenone-treated group): consisted of 6 rats and received a subcutaneous injection of 1.5 mg rotenone/kg b.w. dissolved in 5ml DMSO/kg b.w., once every 2 days for 2 weeks[9,10].

Group C (BM-MSCs-treated group): consisted of 6 rats. They were injected with rotenone of the same route, duration and regimen as in group B followed by a once intraperitoneal injection of a flask of one million heterogeneous BM-MSCs diluted with 1 ml of saline loaded in a 1 ml sterile syringe/rat[11]. The injection was done slowly to prevent the obstruction of the needle[8].

At the end of the experiment, the animals were weighed again then anaesthetized by ether inhalation and perfused in the left ventricle by normal saline injection. The rats of group A1 and group B were sacrificed after 2 weeks of administration of chemicals. The rats of group A2 were sacrificed after 5 weeks of administration of DMSO. The rats

of group C were sacrificed 3 weeks after BM-MSCs injection (after 5 weeks from the onset of the experiment)[8]. The brains were extracted and weighed. The specimens were exposed to the following studies:

Histological techniques

Sections were stained with Haematoxylin and Eosin stain (H&E) to study the nuclei and cytoplasm. Semithin sections were stained with toluidine blue and examined by light microscopy. Ultrathin sections were stained with uranyl acetate and lead citrate and then examined by transmission electron microscope.

Immunohistochemistry

1. Glial fibrillary acidic protein (GFAP) was used to identify neuro-inflammatory reactions.
2. Caspase-3 was used to evaluate the apoptotic processes.
3. Ubiquitin immunostaining was used to detect any abnormally aggregated proteins.

Preparation of paraffin sections according to Alturkistani et al.[12]

The brain was fixed in a 10% buffered formalin solution. The fixed tissues were trimmed into appropriate sizes and placed in embedding cassettes. The paraffin embedding schedule was done as follows:70% ethanol, two changes; 1 hour each, 80% ethanol, one change; 1 hour, 95% ethanol, one change; 1 hour, 100% ethanol, three changes; 1.5 hours each, xylene, or xylene substitute, three changes; 1.5 hours each, Paraffin wax (58-60ºC), two changes; 2 hours each. Embedding of the tissues into paraffin blocks was done in pure hard paraffin (melting point: 58-60°C). Paraffin ribbons were placed in a water bath at 40-45ºC. The sections were put onto slides, allowed to dry in the air for 30 minutes and baked in a 45-50ºC oven overnight. The sections were deparaffinized in 2-3 changes of xylene, 10 minutes each. Hydration was done in 2 changes of 100% ethanol each for 3 minutes, and 95% and 80% ethanol each for 1 minute. Washing with distilled water was done at last. The paraffin blocks containing the specimens were cut serially in the coronal planes (8-10µ thick).

Tissue processing for electron microscopic study according to Suvarna et al.[13]

Brain tissue was dissected at about $3mm^3$ to allow electrons to pass right through the sample. Primary fixation was done in 2.5% glutaraldehyde and 4% formaldehyde for 2 hours at room temperature. Fixed tissue was washed in distilled water (DH_2O) 3 times in 10-minute changes. Post-fixation was done in 1% osmium tetroxide for 1 hour. Fixed tissue was washed out in DH_2O 3 times for 10-minute changes. The dehydration series was done as follows: 30% ethanol for 10 minutes, 50% ethanol for 10 minutes, 70% ethanol for 10 minutes, 90% ethanol for 10 minutes and 100% ethanol for 10 minutes, respectively. Samples were embedded in fresh resin and cured overnight at 60ºC. The sectioning process was done to produce thin slices of a specimen which were cut by an ultramicrotome with a diamond knife to produce ultrathin sections 60-90 nm thick. The sections were stained for several minutes using a double staining technique, with an aqueous or alcoholic solution of uranyl acetate followed by an aqueous lead citrate. The sections were observed with the transmission electron microscope (TEM) ("Jeol" E.M.-100 CX11; Japan) at the Electron Microscopic Unit of Assiut University.

Immunohistochemistry according to Cattoretti et al.[14]

Immunohistochemical studies were performed using primary mouse anti-GFAP antibody, primary rabbit anti-rat caspase-3 antibody and monoclonal anti-ubiquitin antibody respectively. After fixation in 10% neutral-buffered formalin for 2 days, the specimens were dehydrated, cleared, and embedded in paraffin. The paraffin sections were cut at 5µ and mounted on coated slides. The slides were treated with 0.01 mol/l citrated buffer (pH 6.0) for 10 minutes to unmask the antigen. The sections were incubated in 0.3% H_2O_2 for 30 minutes to eliminate endogenous peroxidase activity before blocking with 5% horses' serum for 2 hours at room temperature to inhibit the non-specific immunoreactions. Slides were incubated with primary antibody 1:100 monoclonal mouse anti-GFAP, 1:100 polyclonal rabbit anti-caspase-3 and 1:100 monoclonal mouse anti-ubiquitin (Thermo Scientific Company, USA) at 4ºc for 18-20 hours washed and incubated with biotinylated secondary antibodies and then with 0.05% diaminobenzidine. The slides were then counterstained with Myer´s Haematoxylin, dehydrated, cleared, and mounted. GFAP-positive astrocytes appeared brown, including their bodies and processes, while a positive reaction to caspase-3 was visualized as a brown colouration of the cytoplasm of the neural cells. A positive reaction to ubiquitin was visualized as brownish fibrils masking the cytoplasm. Negative control experiments were performed by incubating the slides without primary antibody; hence, no immunostaining occurred.

Morphometric measurements and statistical analysis

Statistical analysis was done using IBM SPSS Statistics version 21 (SPSS Inc., Chicago, IL, USA). Collected data (body and brain weights of the different studied groups) were represented as means ± SD and tested for normality using the Shapiro-Wilkes test. As data were normally distributed, the student`s t-test was used to compare 2 different groups and the paired t-test was used for the comparison of variables before and after treatments. In both statistical tests, *p-values* < 0.05 were considered statistically significant.

RESULTS

Morphological results

Regarding body weight, a statistically significant decrease in the body weight of the rotenone-treated rats (Group B) was detected in comparison to

their corresponding aged control rats (Group A1) (*p-value* < 0.05). On the other hand, no statistically significant difference was detected between the body weights of the rotenone-treated rats (Group B) and the stem cells-treated rats (Group C) (p-value =0.202). There was a highly statistically significant decrease in the body weight of the stem cells-treated rats (Group C) compared to their corresponding age control rats (Group A2) (*p-value* < 0.001) (Tables 1-3).

Regarding brain weight, a statistically significant increase in the brain weight of the rotenone-treated rats (Group B) was detected in comparison to their corresponding aged control rats (Group A1) (*p-value* < 0.05). In addition, there was a statistically significant increase in the brain weight of the stem cells-treated rats (Group C) in comparison to the rotenone-treated rats (Group B) (*p-value* < 0.05). There was a highly statistically significant increase in the brain weights of stem cells-treated rats (Group C) in comparison to their corresponding aged control rats (Group A2) (*p-value* < 0.001) (Tables 4-6).

Histological results

There was no obvious histological difference between the control groups (Group A1 and Group A2) throughout the experiment.

Light microscopic results

A) Control group (Group A): The light microscopic results using H&E and toluidine blue stain of the SN field of the control animals demonstrated a cell-rich band full of dopaminergic neurons, SNpc and a cell-poor SNpr The dopaminergic neurons of SNpc were lightly stained, linearly distributed, fusiform and arranged in the form of a band abundant in neurons of different sizes, with pale vesicular nuclei and prominent nucleoli. Their cytoplasm was granular and basophilic. The midbrain showed a red nucleus as well as the basis pedunculi (Figures 2a,d,g,3a).

B) Rotenone-treated group (Group B): The light microscopic results using H&E and toluidine blue stain of the SN field of the rotenone-treated rats demonstrated that SNpc was less dense with marked neuronal loss. Aggregates of Lewy bodies were detected in the form of eosinophilic patches scattered within the field. Dopaminergic neurons were darkly stained, irregularly outlined and apoptotic. Some dopaminergic neurons were surrounded by pericellular halos. The nuclei were dark and condensed with ill-defined nucleoli. The red nucleus was replaced by damaged nerve fibres. Some blood vessels were distorted and congested while others showed perivascular cuffing with mononuclear cells. The field was infiltrated with microglial cells (Figures 2b,e,h,3b).

C) Stem cells-treated group (Group C): The light microscopic results using H&E and toluidine blue stain of SN field of the stem cells-treated animals demonstrated that some dopaminergic neurons of the SNpc were small, rounded and irregularly distributed and the absence of the eosinophilic patches. However, some neurons were large and fusiform. The cytoplasm of these neurons was basophilic. Neurons of the red nucleus showed a small number of proliferating neurons. Residual blood vessels revealing perivascular cuffing with mononuclear cells were observed (Figures 2c,f,i,3c).

Electron microscopic results

A) Control group (Group A): The ultrastructure of the control group demonstrated that the dopaminergic neurons were fusiform with a clear regular outline. Their nuclei were oval, euchromatic with a clear nuclear envelope and prominent nucleoli. The cytoplasm was granular and full of organelles. Numerous mitochondria, as well as free ribosomes and rough endoplasmic reticulum, were observed. Pigmented organelles of neuromelanin and myelinated nerve fibres were recognized (Figures 4a,d).

B) Rotenone-treated group (Group B): The ultrastructure of the rotenone-treated group demonstrated that dopaminergic neurons had irregular, heterochromatic and shrunken nuclei with small nucleoli. The cytoplasm showed a marked reduction of the cell organelles. Numerous lysosomes as well as swollen mitochondria were detected. Marked rarefaction and intracellular vacuolization appeared within the dopaminergic cells (Figures 4b,e,f). A Lewy body with a destroyed, ill-defined membrane and irregular dark pigments surrounded by areas of rarefaction was seen (Figure 4g). Adjacent dividing microglia with the typical structure of dense heterochromatin lining the nuclear membrane, a narrow rim of contrasting light cytoplasm and microglial processes were noticed (Figure 4h).

C) Stem cells-treated group (Group C): The ultrastructure of the stem cell-treated group demonstrated that dopaminergic neurons had a quite regular fusiform outline. The nuclei were euchromatic with an invaginated nuclear envelope. The cytoplasm showed restored cell organelles, numerous mitochondria, free ribosomes, and rough endoplasmic reticulum. Dispersed pigmented organelles of neuromelanin and a few areas of residual rarefaction were detected (Figures 4c,i).

Immunohistochemistry

GFAP

GFAP immunohistochemical staining of the control group (Group A) revealed a weak positive immune reaction (Figure 5a). In contrast, the rotenone-treated group (Group B) demonstrated a strong positive GFAP-immune reaction and hypertrophied astrocytes (Figure 5b). Regarding the stem cells-treated rat (Group C), a moderate positive GFAP-immunoreaction was detected (Figure 5c).

Caspase-3

Caspase-3 immunohistochemical staining of the control group (Group A) revealed a weak positive caspase-3-immune reaction (Figure 5d). In contrast, the rotenone-treated group (Group B) demonstrated a strong positive

caspase-3-immune reaction (Figure 5e). Regarding the stem cells-treated rats (Group C), the field showed a moderate positive caspase-3-immune reaction (Figure 5f).

Ubiquitin

Ubiquitin immunohistochemical staining of SN in the control group (Group A) revealed a weak positive ubiquitin-immunoreactivity in the form of brownish deposits (Figure 5g). In contrast, the rotenone-treated group (Group B) demonstrated a strong positive ubiquitin-immunoreactivity in the form of brownish deposits as well as irregular plaques (Figure 5h). Regarding the stem cells-treated rats (Group C), the field showed a moderate positive ubiquitin-immunoreactivity (Figure 5i).

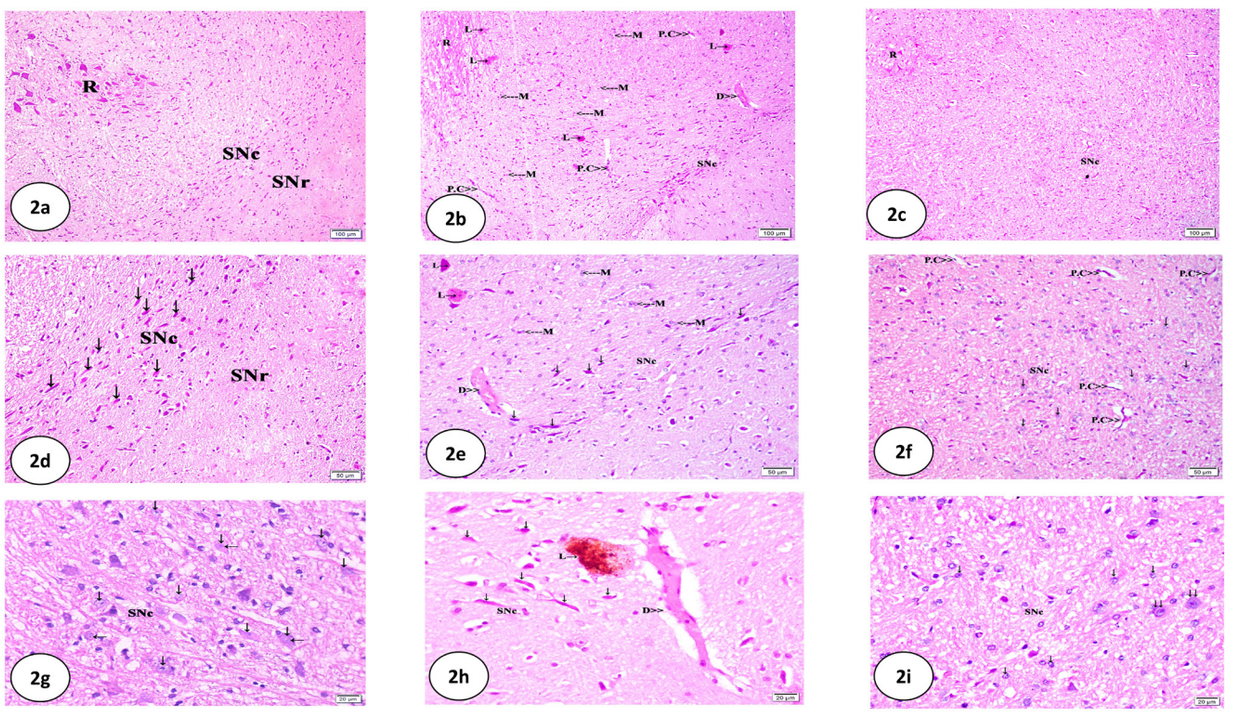

Fig.2

Fig. 2: H&E-stained photomicrographs of a transverse section of the midbrain of the adult rats of studied groups. The control group (Figs. 2a,2d&2g) shows a red nucleus (R), SNpc (SNc) rich in dopaminergic neurons (↓) and SNpr (SNr) poor in dopaminergic neurons. The dopaminergic neurons (↓) are of different sizes, lightly stained, linearly distributed, and fusiform. They reveal pale vesicular nuclei (←) with prominent nucleoli and granular and basophilic cytoplasm. The rotenone-treated group (Figs. 2b,2e&2h) shows damaged red nucleus (R), less dense SNpc (SNc) with apparent neuronal loss, darkly stained dopaminergic neurons (↓), distorted congested blood vessel (D>>), perivascular cuffing with mononuclear cells (P.C>>), microglial cells (<---M) and aggregates of Lewy bodies (L→). The stem cells-treated group (Figs. 2c,2f&2i) shows proliferating neurons of the red nucleus (R) and SNpc (SNc) and the absence of the eosinophilic patches. Dopaminergic neurons (↓) of SNc were small, rounded and irregularly distributed. Residual blood vessels exhibit perivascular cuffing with mononuclear cells (P.C>>). Some dopaminergic neurons appear large and fusiform with basophilic cytoplasm (↓↓). (H&E; 2a-2c; X100, 2d-2f; X200 and 2g-2i; X400)

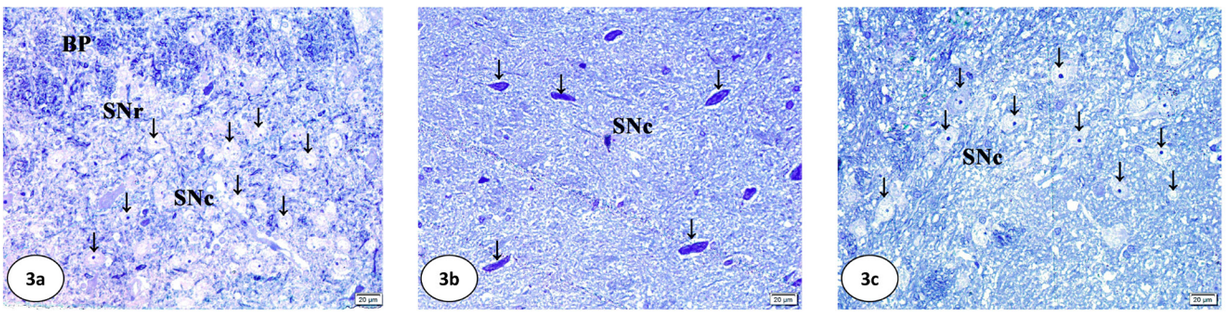

Fig. 3: Toluidine blue-stained photomicrographs of semithin sections of the midbrain of the adult rats. The control group (Fig. 3a) shows SNpc (SNc) and SNpr (SNr) as well as basis pedunculi (BP). SNpc (SNc) has abundant fusiform lightly stained dopaminergic neurons (↓) of different sizes with pale nuclei and prominent nucleoli. The rotenone-treated group (Fig. 3b) shows SNpc (SNc) with marked neuronal loss and apoptotic dopaminergic neurons with darkly stained nuclei and pericellular haloes (↓). The stem cells-treated group (Fig. 3c) shows SNpc (SNc) with small rounded and fusiform dopaminergic neurons (↓). (Toluidine blue ; X400)

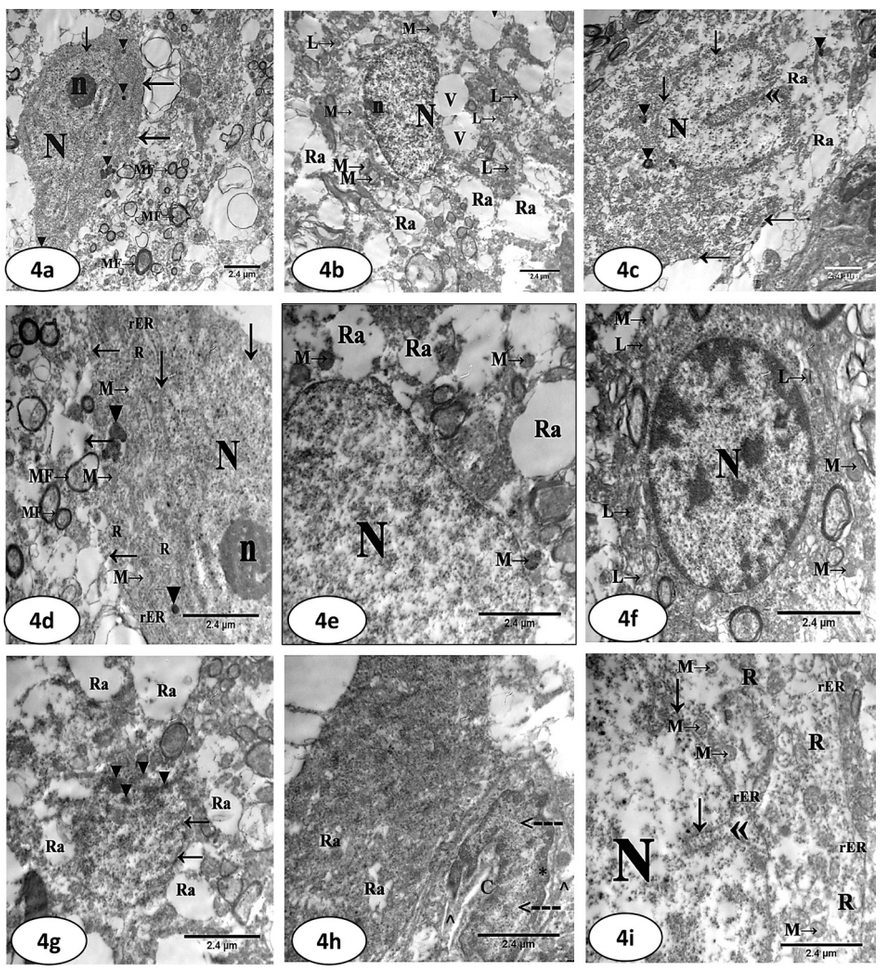

Fig. 4: Electron photomicrographs of the dopaminergic neurons of the adult rats of studied groups. The control group (Fig. 4a&4d) shows a fusiform cell with a clear regular outline (←), an oval euchromatic nucleus (N) with a clear nuclear envelope (↓) and a prominent nucleolus (n). Pigmented areas of neuromelanin (▼), myelinated nerve fibres (MF→), numerous mitochondria (M→), free ribosomes (R) and rough endoplasmic reticulum (rER) are observed. The rotenone-treated group (Figs. 4b,4e,4f,4g&4h) shows a shrunken heterochromatic irregular nucleus (N) with a small nucleolus (n), lysosomes (L→), swollen mitochondria (M→), rarefaction (Ra) and intracellular vacuolization (V) (Figs. 4b,4e&4f). A Lewy body shows a destructed ill-defined membrane (←) and irregular dark pigments (▼) surrounded by areas of rarefaction (Ra) (Fig. 4g). Areas of rarefaction (Ra) and adjacent dividing microglia (<---) with dense heterochromatin lining the nuclear membrane (*), a narrow rim of contrasting light cytoplasm (C) and microglial processes (^) are observed (Fig. 4h). The stem cells-treated group (Figs. 4c&4i) shows euchromatic dopaminergic nucleus (N), clear nuclear envelope (↓) with nuclear invagination («), pigmented organelles of neuromelanin (▼) and residual areas of rarefaction (Ra). A quite regular fusiform outline (←) of the neuron is observed. Numerous mitochondria (M→), free ribosomes (R) and rough endoplasmic reticulum (rER) are noticed. (TEM, Figs. 4a-4c; X4800, Figs. 4d-4i; X10000)

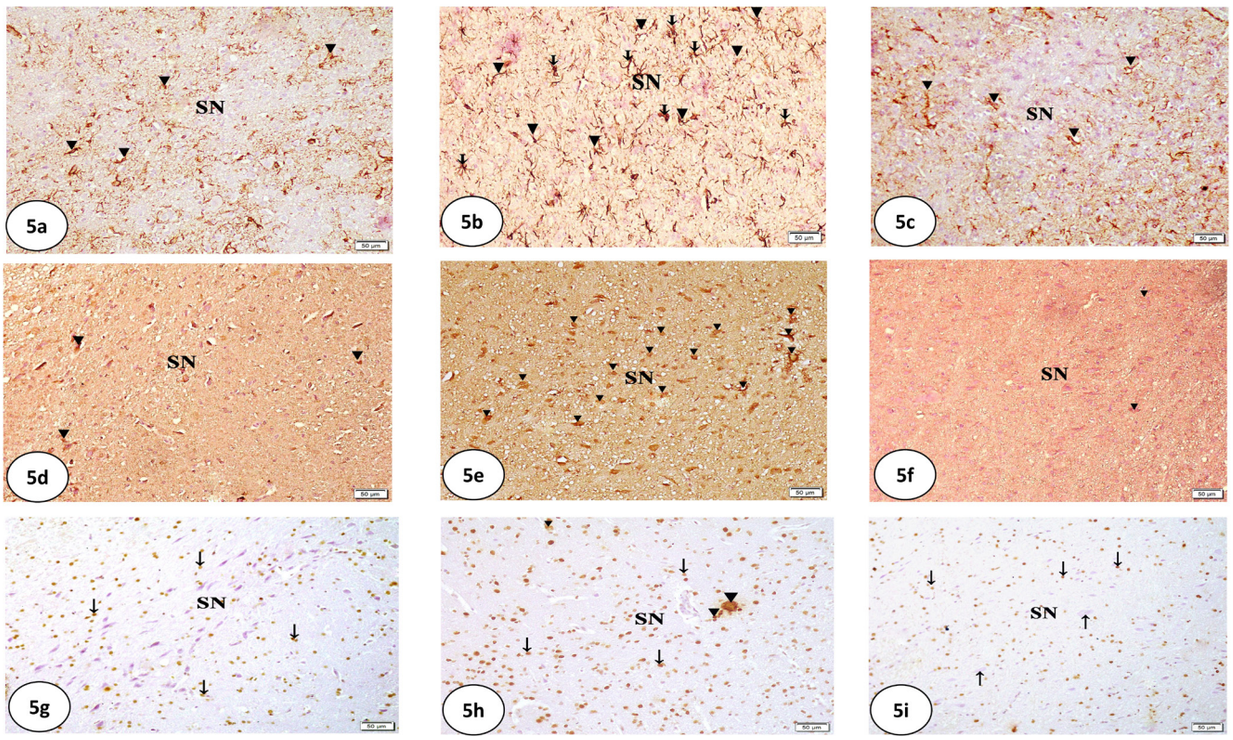

Fig. 5: Immunohistochemical photomicrographs of the substantia nigra (SN) of the studied groups. The control group shows a weak positive GFAP-immune reaction (▼) (Fig. 5a), a weak positive caspase-3-immunereaction (▼) (Fig. 5d) and a weak positive ubiquitin-immunoreactivity in the form of brownish deposits (↓) (Fig. 5g). The rotenone-treated group shows a strong positive GFAP-immune reaction (▼), hypertrophied astrocytes (↓) (Fig. 5b), a strong positive caspase-3-immune reaction (▼) (Fig. 5e) and a strong positive ubiquitin-immunoreactivity (↓) as well as irregular plaques (▼) (Fig. 5h). The stem cells-treated group shows a moderately positive GFAP-immune reaction (▼) (Fig. 5c), a moderately positive caspase-3-immune reaction (▼) (Fig. 5f) and a moderate positive ubiquitin-immunoreactivity (↓) of the dopaminergic neurons (↑) (Fig. 5i). (GFAP immunohistochemical staining, Figs. 5a-5c; Caspase-3 immunohistochemical staining, Figs. 5d-5f; Ubiquitin immunohistochemical staining, Figs. 5g-5i; X200)

Table 1: Comparison between the body weights of the rotenone-treated rats (Group B) and the corresponding aged control rats (Group A1).

	Body weight (gm) of Group B	Body weight (gm) of Group A1	*P-value*
Mean ± SD	144.2 ± 32.5	219.6 ± 6.7	0.04*

SD: Standard deviation — Student`s t-test was used — *Statistically significant

Table 2: Comparison between the body weights of the rotenone-treated rats (Group B) and stem cells-treated rats (Group C).

	Body weight (gm) of Group B	Body weight (gm) of Group C	*P-value*
Mean ± SD	144.2 ± 32.2	154.8 ± 15.2	0.202□

SD: Standard deviation — Paired t-test was used — □Not statistically significant

Table 3: Comparison between the body weights of stem cells-treated rats (Group C) and the corresponding aged control rats (Group A2).

	Body weight (gm) of Group C	Body weight (gm) of Group A2	*P-value*
Mean ± SD	154.8 ±15.2	227.3 ± 13.5	0.002**

SD: Standard deviation — Student`s t-test was used — **Highly statistically significant, *p-value*<0.01

Table 4: Comparison between the brain weights of the rotenone-treated rats (Group B) and the corresponding aged control rats (Group A1).

	Body weight (gm) of Group B	Body weight (gm) of Group A1	*P-value*
Mean ± SD	2085.3 ± 216.5	1845.8 ± 117.3	0.038*

SD: Standard deviation — Student`s t-test was used — *statistically significant, *p-value*<0.05

Table 5: Comparison between brain weights of the rotenone-treated rats (Group B) and stem cells-treated rats (Group C).

	Body weight (gm) of Group B	Body weight (gm) of Group C	*P-value*
Mean ± SD	2085.3 ± 216.5	2412.2 ± 25	0.012*

SD: Standard deviation | Paired t-test was used | *statistically significant

Table 6: Comparison between the brain weights of stem cells-treated rats (Group C) and the corresponding aged control rats (Group A2).

	Body weight (gm) of Group C	Body weight (gm) of Group A2	*P-value*
Mean ± SD	2412.2 ± 25	2060.2 ± 121.2	0.001**

SD: Standard deviation | *Student`s t-test was used | *Highly statistically significant

DISCUSSION

The neurodegenerative diseases are incurable and debilitating conditions that result in progressive degeneration and successive death of the nerve cells[15]. Stem cell therapy is considered to be a successful line of treatment in neurodegenerative animal models[16]. The present study has selected MSCs for transplantation as they are easily accessible, with no risk of rejection, and can be obtained from various tissues such as bone marrow, umbilical cord, and adipose tissue[17].

The reduction in the body weight of rotenone-treated rats (Group B) observed in the present study was in agreement with Akinmoladun *et al*.[18]. It is well-known that rotenone produces serious hepatic and renal damage that results in systemic toxicity accompanied by weight loss[19]. The repeated rotenone treatment is thought to induce a state of repeated energy stress which progressively decays the cells' energy production ability and makes them more sensitive to energy stress. A turnover process in the glycogen and fat body stores takes place to obtain energy. In addition, rotenone produces a state of lipid peroxidation that leads to an increase in membrane permeability and loss of body fluidity, thus in turn loss of weight[20]. In contrast, Ma *et al*.[21] reported that rats' weight remained stable after a single intravenous injection of MSCs and the sacrifice of the rats one week later. Their study demonstrated that MSCs could even reduce liver fat and glycogen content, which might account for no improvement of the weight of the rotenone-treated rats in the present study. These different results from the present ones could be attributed to the different methodologies that were applied.

Regarding brain weight, the rotenone-treated rats (Group B) in the present study showed a significant increase in brain weight as compared to their corresponding control ones. This comes in line with Akinmoladun *et al*.[18]. Stephens *et al*.[22] and Ramalingam *et al*.[23] documented that rotenone treatment induces neurite degradation with the presence of intraneuronal alpha-synuclein Lewy-body accumulations in the brain tissue[24]. With the larger alpha-synuclein accumulations in some neurons, the increase in brain weight in the present work could be explained.

The present work showed a significant increase in brain weight even after injection of rotenone-treated rats with BM-MSCs. This could be explained as a continuous exaggerated form of rotenone toxicity which might exceed the regenerative power of MSCs. This conflicts with the histological results of our study that demonstrated a noticeable improvement with BM-MSCs treatment. The possible justification for this increase in brain weight is to be an actual form of recovery. Ramalingam *et al*.[23] pointed out that after treatment of the diseased rats with BM-MSC, cell numbers markedly increased as well as accompanied removal of the brain protein accumulations. The neurite outgrowth was mainly composed of cytoskeletal neurofilaments and microtubules which share in the new brain tissue formation as reported by the researchers. This effective process of regeneration and restoration might justify the increase in the brain weight of group B with the obvious histological elimination of the brain tissue from the Lewy bodies in the present study. Furthermore, the significant increase in the brain weight of group C in comparison to the corresponding control ones can be easily explained in the same manner.

The present histological effect of rotenone on the substantia nigra was in agreement with the study of Siracusa *et al*.[25] and Fikry *et al*.[26]. The findings of the present work as the dark nuclei, the ill-defined nucleoli, and even the pericellular halos, are all known as hallmarks of degeneration as considered by Yuceli *et al*.[27]. Blood vessels of the present study were distorted and congested and showed perivascular cuffing with mononuclear cells and this was reported by Yuceli *et al*.[27] who declared that these findings were accompanied by activation of microglial cells. Microglial infiltration was justified in our study as a sign of the neuroinflammatory process[27]. Subhramanyam *et al*.[28] postulated that microglia are activated to secrete either proinflammatory factors that enhance cytotoxicity or anti-inflammatory neuroprotective factors that assist in wound healing and tissue repair. Excessive microglial activation damages the surrounding healthy neural tissue and the factors secreted by the dead or dying neurons exacerbate in turn the chronic activation of microglia, causing more neuronal loss[28].

The present work showed a great neuronal loss of the SN dopaminergic neurons and red nucleus. This corresponds to the previous study by Zhang *et al*.[29]. Dopaminergic neurons in the SN are known to be highly

susceptible to oxidative damage. Rotenone produces high mitochondrial ROS with resultant degeneration of dopaminergic neurons, favouring cell death. Furthermore, ROS initiate inflammatory pathways extending the deleterious milieu for the remaining vulnerable neurons. Indeed, both oxidative stress and inflammation are possible mechanisms contributing to neuronal degeneration in PD, as reported by Liu and Cheung[30] and Fikry *et al*.[26].

The Lewy bodies observed in midbrain tissue in the rotenone-treated group of the present study are in agreement with Patrick and Jennifer[31]. Rotenone induces alpha-synuclein aggregation-the primary structural component of Lewy body fibrils- due to impairment of the autophagy process as declared by Graciela *et al*.[32] and Mahesh *et al*.[24].

The ultrastructural results of the present study were in line with those of the present light microscopic study. The dopaminergic neurons of the rotenone-treated group in the present study were of an ill-defined cell membrane. The pale nucleoli, the rarefied cytoplasm, the marked reduction of the cell organelles as well as the increase in lysosomal number, were in agreement with the neurodegenerative effect of the rotenone as reported by Siracusa *et al*.[25].

The observed intracellular cytoplasmic vacuolization of the cells in the rotenone-treated rats of the present work could be due to its cytotoxic effect as it acts as a vacuolization inducer, as mentioned by Park and Ellis[33]. The present study demonstrated swollen mitochondria, which were a sign involved in the context of PD pathology, as reported by Siracusa *et al*.[25]. Mitochondrial dysfunction is considered a primary cause of PD. Early dysfunction of the mitochondrial electron transport chain complex-I could account for PD pathology. In rotenone-induced PD rats, peroxisome proliferator-activated receptor gamma coactivator-1α, a strong stimulator of mitochondrial biogenesis, is markedly downregulated. Added to that, rotenone decreases ATP levels and even mitochondrial structural damage, such as the disruption and dissolution of mitochondrial cristae[34].

Regarding stem cell therapy, a histological improvement in the PD rats was observed in the present work after BM-MSCs therapy. Researchers[3,16] postulated that those cells are capable of self-renewal, proliferation, differentiation, and transformation into different types of central nervous system neurons and glial cells. Added to that, the stem cells secrete neurotrophic factors to provide a protective environment for endogenous cells. These factors protect the regenerated neurons against stress-induced apoptosis[23,35].

The role of stem cell therapy in PD in the present work was observed in many aspects. Neuronal proliferation was evidenced in the increase in dopaminergic neurons of SNpc and a small number of proliferating neurons appeared in the red nucleus. This improvement in the PD study was in line with the assumptions of studies by Ebrahimi *et al*.[36], Xu *et al*.[37], Abdelwahab *et al*.[38] and Liu and Cheung[30].

Abdelwahab *et al*.[38] have documented a significant increase in the mean level of dopamine in rotenone-treated rats after BM-MSCs therapy. Moreover, Xu *et al*.[37] praised the ability of those cells to promote neural cell survival and regeneration, repair affected neurons, and synthesize and release neurotrophic factors and neurotransmitters. In addition, MSCs not only alleviate PD through their antiapoptotic anti-inflammatory and neuroprotective effects, but also improve alpha synuclein-induced neuron degeneration as mentioned by Liu and Cheung[30]. They added that the MSCs-derived neurons can survive, grow their axons that innervate the brain and support functional recovery from neurotoxin-induced motor deficits.

The stem cells-treated group (Group C) of the present study demonstrated restoration of euchromatic nuclei, clear nuclear envelope, increase in cell organelles as well as excess-free ribosomes, which were all in line with the regeneration process. This confirmed the previous stem cell studies of Liu *et al*.[16]. The present study of group C demonstrated nuclear envelope invagination, which could be a sign of nuclear activity, as reported by Liu *et al*.[16]. They mentioned that the formation of such invaginations could provide more anchoring sites for active genes and enhance gene expression promoting nuclear activity. Moreover, the MSCs have the potential to compensate for mitochondrial malfunctions through a process of mitochondrial transfer between MSCs and ageing cells as mentioned by Liu *et al*.[39] and Nzigou *et al*.[40].

Regarding the immunohistochemical results using GFAP (a marker for astrocytes), the rotenone-treated group of the present work showed a strong positive GFAP-immunoreaction. In regards to stem cell-treated rats, there was a moderate positive GFAP-immunoreaction compared to the rotenone-treated group. This was in agreement with Andrzejewska *et al*.[41]. The observed gliosis of the rotenone-treated group in the present work as expressed by the strong positive GFAP-immunoreaction could explain the resulting astrocytosis. Normally, astrocytes provide trophic support for neurons and synapses. After a brain pathology, they undergo a pronounced transformation called 'reactive astrocytosis'. Moreover, the microglia are one of the sources of free radicals in neurodegenerative models[42]. The presence of moderate positive GFAP-immunoreaction after stem cell treatment observed in the present study could be referred to as the ability of the stem cells to differentiate not only into neurons but also into astrocytes[42]. However, the present GFAP immunohistochemical results were against Abdelwahab *et al*.[38] who documented a significant decrease in the number of GFAP-immune positive cells with neurodegenerative disorders and a significant increase in GFAP expression after stem cell therapy which was even higher than the control. The different obtained results may be attributed to the different methodologies they followed as they injected the rats with $2x10^6$ BM-MSCs and sacrificed them 28 days after injection with the stem cells.

By using caspase-3 immunohistochemical staining, the present work showed a strong positive caspase-3-immunoreaction of the rotenone-treated group as compared to the control. This was in the context of neuronal loss in PD[25,27]. As regards the stem cells-treated rats of the present work, the noticed moderate positive caspase-3-immunoreaction was in line with the previously mentioned regenerative role of the stem cells[16,30,43].

By using ubiquitin immunohistochemical staining, the rotenone-treated group of the present work showed a strong positive immunoreaction as well as large irregular plaques as compared with the control. This immunoreactivity was in the context of Watanabe *et al*.[44]. In neurodegenerative diseases, the ubiquitin conjugates contain disease-characteristic proteins such as alpha-synuclein proteins in PD. Accumulation of ubiquitin conjugates reflects the failed attempts by the ubiquitin system to remove these abnormal proteins. However, previous studies have demonstrated that the soluble aggregated abnormal proteins can even inhibit ubiquitin system. Thus, a reduction in the activity of this system leads to the accumulation of proteins, and the mutations of those proteins cause more system failure[45]. As regards the stem cells-treated rats of the present work, there was moderate positive ubiquitin-immunoreaction that was in agreement with the regenerative effect of the stem cells[30].

CONCLUSION

Rotenone has a degenerative impact on the SN which can be ameliorated using bone marrow mesenchymal stem cells.

ETHICAL STATEMENTS

This study was carried out in strict accordance with the International Guidelines for the Care and Use of Laboratory Animals. The experimental protocol was approved by the Ethics Committee at the Faculty of Medicine, Assiut University, (Approval number: IRB17200423).

CONFLICT OF INTERESTS

There are no conflicts of interest.

REFERENCES

1. Zeng X, Geng W, Jia J. Neurotoxin-induced animal models of Parkinson disease: Pathogenic mechanism and assessment. ASN Neuro. 2018; 10:1-15. DOI: 10.1177/1759091418777438.
2. Wang E, Du G, Lewis M, Lee E, De Jesus S, Kanekar S, Kong L, Huang X. Multimodal MRI evaluation of parkinsonian limbic pathologies. Neurobiology of Aging. 2019; 76:194-200. DOI: 10.1016 /j.neurobiolaging.2019.01.004.
3. Mousaei M, Seok J, Park H, Liakath A, Al-Hendy A. Stem Cell Therapy: From Idea to Clinical Practice. International Journal of Molecular Sciences. 2022; 23(5):2850. DOI:10.3390/ijms23052850.
4. Anne E, Monica E, William P, Romina A, Anselme L, Vicki W, Emanuele C, Unai P, Cristina S, Laura J, Cheney D, Steven A, Josep M, Leslie M, *et al*. Translating cell therapies for neurodegenerative diseases: Huntington's disease as a model disorder. Brain. 2022; 145(5):1584-1597. DOI: 10.1093/brain/ awac086.
5. Garcia-Leon J, Vitorica J, Gutierrez A. Use of human pluripotent stem cell-derived cells for neurodegenerative disease modeling and drug screening platform. Future medicinal chemistry. 2019; 11: article (11). DOI: 10.4155/fmc-2018-0520.
6. Cosacak M, Bhattarai P, Kizil C. Alzheimer's disease, neural stem cells and neurogenesis: cellular phase at single-cell level. Neural regeneration research. 2020; 15(5):824-827. DOI: 10.4103/1673-5374.268896.
7. Helena D. A training set for sentences describing temperature housing conditions for mice. Mendeley Data: v3, 2019. DOI: 10.17632/24twm89hsz.3.
8. Abo-Azizaa F, Zaki A, Abo El-Maaty A. Bone marrow-derived mesenchymal stem cell (BM-MSC): A tool of cell therapy in hydatid experimentally infected rats. Cell Regeneration. 2019; 8:58-71. DOI: 10.1016/j. cr.2019.11.001.
9. Chernivec E, Cooper J, Naylor K. Exploring the effect of rotenone-a known inducer of Parkinson's disease-on mitochondrial dynamics in Dictyostelium discoideum. Cells. 2018; 7(11):201. DOI: 10.3390/cells7110201.
10. Abdel-Salam O, El-Shamarka M, Omara E. Grape seed extract exerts an anti-apoptotic effect and attenuates the decrease in striatal tyrosine hydroxylase in rotenone-treated mice. Reactive Oxygen Species. 2019; 7(19):30-46. DOI:10.20455/ros.2019.805
11. Marzban M, Mousavizadeh K, Bakhshayesh M, Vousooghi N, Vakilzadeh G, Torkaman-Boutorabi A. Effect of multiple intraperitoneal injections of human bone marrow mesenchymal stem cells on cuprizone model of multiple sclerosis. The Iranian Biomedical Journal. 2018; 22(5):312-321. DOI: 10.29252/ ibj.22.5.312.
12. Alturkistani H, Tashkandi F, Mohammed S. Histological Stains: A literature review and case study. Global Journal of Health Science. 2016; 8(3):72-79. DOI: 10.5539/gjhs. v8n3p72.
13. Suvarna S, Layton C, Bancroft J. Bancroft's Theory and Practice of Histological Techniques E-Book: Expert. Churchill Livingstone, Elsevier, China. 2018; 8th edition. Hardback eBook ISBN: 9780702068645. 9 7 8 - 0 - 7 0 2 0 - 6 8 6 4 – 5. ISBN: 9780702068867.
14. Cattoretti G, Pileri S, Parravicini C, Becker M, Poggi S, Bifulco C, Key G, D'Amato L, Sabattini E, Feudale E, Reynolds F, Gerdes J, Rilke F. Antigen unmasking on formalin-fixed, paraffin-embedded tissue sections. The Journal of Pathology. 1993; 171(2):83-98. DOI: 10.1002/path.1711710205.

15. Bekhedda H, Norredine M, Abbassia D, Abdelaziz G, Hicham M. Histological study of the effects of aluminum chloride exposure on the brain of wistar rats female. Journal of Drug Delivery and Therapeutics. 2020; 10(3-s):37-42. DOI:10.22270/jddt.v10i3-s.4152

16. Liu X, Yang L, Zhao L. Stem cell therapy for Alzheimer's disease. World Journal of Stem Cells. 2020; 12(8):787-802. DOI: 10.4252/wjsc.v12.i8.787.

17. Andrzejewska A, Lukomska B, Janowski M. Concise Review: Mesenchymal Stem Cells: From Roots to Boost. Stem Cells. 2019; 37(7):855-864. DOI: 10.1002/stem.3016.

18. Akinmoladun A, Olaniyan O, Famusiwa C, Josiah S, Olaleye M. Ameliorative effect of quercetin, catechin and taxifolin on rotenone-induced testicular and splenic weight gain and oxidative stress in rats. Journal of Basic and Clinical Physiology and Pharmacology. 2020; 31(3): e20180230. DOI: 10.1515/jbcpp-2018-0230.

19. Afzal M, Kazmi I, Quazi A, Ahmad A, Al-Abaasi F, Imam F, Alharbi K, Alzarea S, Zafar A. 6-Shogaol attenuated ethylene glycol and aluminium chloride induced urolithiasis and renal injuries in rodents. Saudi Journal of Biological Sciences. 2021; 28(6):3418-3423. DOI: 10.1016/j.sjbs.2021.03.005.

20. Mbiydzenyuy N, Ninsiima H, Valladares M, Pieme C. Zinc and linoleic acid pre-treatment attenuates biochemical and histological changes in the midbrain of rats with rotenone-induced Parkinsonism. BMC Neuroscience. 2018; (19): Article number: 29. DOI: 10.1186/s12868-018-0429-9.

21. Ma Y, Wang L, Yang S, Liu D, Zeng Y, Lin L, Qiu L, Lu J, Chang J, Li Z. The tissue origin of human mesenchymal stem cells dictates their therapeutic efficacy on glucose and lipid metabolic disorders in type II diabetic mice. Stem Cell Research & Therapy. 2021; 12:385. DOI: 10.1186/s13287-021-02463-x.

22. Stephens A, Zacharopoulou M, Schierle G. The cellular environment affects monomeric α-synuclein structure. Trends in Biochemical Sciences 2019; 44(5):453-466. DOI: 10.1016/j.tibs.2018.11.005.

23. Ramalingam M, Jang S, Jeong H. Neural-induced human adipose tissue-derived stem cells conditioned medium ameliorates rotenone-induced toxicity in SH-SY5Y cells. International Journal of Molecular Sciences. 2021; 22(5):2322. DOI: 10.3390/ijms22052322.

24. Mahesh R, Han-Seong J, Jinsu H, Hyong-Ho C, Byeong C, Eungpil K, Sujeong J. Autophagy Signaling by Neural-Induced Human Adipose Tissue-Derived Stem Cell-Conditioned Medium during Rotenone-Induced Toxicity in SH-SY5Y Cells. International Journal of Molecular Sciences. 2022; 23(8): 4193. DOI: 10.3390/ijms23084193.

25. Siracusa R, Scuto M, Fusco R, Trovato A, Ontario M, Crea R, Di Paola R, Cuzzocrea S, Calabrese V. Anti-inflammatory and anti-oxidant activity of Hidrox in rotenone-induced Parkinson's disease in mice. Antioxidants. 2020; 9(9):824. DOI: 10.3390/antiox9090824.

26. Fikry H, Saleh L, Abdel Gawad S. Neuroprotective effects of curcumin on the cerebellum in a rotenone-induced Parkinson's Disease Model. CNS Neuroscience & Therapeutics. 2022; 28: 732-748. DOI: 10.1111/cns.13805.

27. Yuceli S, Naz Yazici G, Mammadov R, Suleyman H, Kaya M, Ozdogan S. The effect of Rutin on experimental traumatic brain injury and edema in rats. In *Vivo*. 2020; 34(5):2453-2460. DOI: 10.21873/in*vivo*.12060.

28. Subhramanyam C, Wang C, Hu Q, Dheen S. Microglia-mediated neuroinflammation in neurodegenerative diseases. Seminars in Cell & Developmental Biology. 2019; 94:112-120. DOI: 10.1016/j.semcdb.2019.05.004.

29. Zhang W, Sun C, Shao Y, Zhou Z, Hou Y, Li A. Partial depletion of dopaminergic neurons in the substantia nigra impairs olfaction and alters neural activity in the olfactory bulb. Scientific Reports. 2019; 9:254. DOI: 10.1038/s41598-018-36538-2.

30. Liu Z, Cheung H. Stem cell-based therapies for Parkinson disease. International Journal of Molecular Sciences. 2020; 21(21):8060. DOI: 10.3390/ijms21218060.

31. Patrick A, Jennifer E. The Molecular and Clinical Pathology of Neurodegenerative Disease, Chapter 3-Parkinson's Disease, Academic Press. 2019; 83-121. DOI: 10.1016/C2015-0-06542-X.

32. Graciela M, Eduardo E, Gabriela B. Handbook of Clinical Neurology, Chapter 16: Lewy bodies in the olfactory system and the hypothalamus, Elsevier. 2021; 182:235-244. DOI: 10.1016/B978-0-12-819973-2.00016-2.

33. Park H, Ellis A. Dietary antioxidants and Parkinson's disease. Antioxidants. 2020; 9:570. DOI: 10.3390/antiox9070570.

34. Angelova P, Barilani R, Lovejoy M, Dossena C, Viganò M, Seresini M, Abramov A. Mitochondrial dysfunction in Parkinsonian mesenchymal stem cells impairs differentiation. Redox Biology. 2018; 14:474-484. DOI: 10.1016/j.redox.2017.10.016

35. Hiller B, Marmion D, Thompson C, *et al*. Optimizing maturity and dose of iPSC-derived dopamine progenitor cell therapy for Parkinson's disease. npj Regenerative Medicine. 2022; 7: 24. DOI: 10.1038/s41536-022-00221-y.

36. Ebrahimi V, Eskandarian Boroujeni M, Aliaghaei A, Abdollahifar M, Piryaei A, Haghir H, Sadeghi Y. Functional dopaminergic neurons derived from human chorionic mesenchymal stem cells ameliorate striatal atrophy and improve behavioral deficits in Parkinsonian rat model. The Anatomical Record. 2020; 303:2274-2289. DOI: 10.1002/ar.24301.

37. Xu H, Zhang J, Tsang K, Yang H, Gao W. Therapeutic potential of human amniotic epithelial cells on injuries and disorders in the central nervous system. Stem Cells International. 2019; (2019):5432301. DOI: 10.1155/2019/5432301.

38. Abdelwahab S, Elsebay S, Gaber F, Abdel-Hafez M, SM N. Comparative study between bone marrow mesenchymal stem cell and their conditioned medium in the treatment of rat model of Parkinsonism. Journal of Cellular Physiology. 2020; 236:440-457. DOI: 10.1002/jcp.29872.

39. Liu K, Zhou Z, Pan M, Zhang L. Stem cell-derived mitochondria transplantation: A promising therapy for mitochondrial encephalomyopathy. CNS Neuroscience & Therapeutics. 2021; 27:733-742. DOI: 10.1111/cns.13618.

40. Nzigou Mombo B, Gerbal-Chaloin S, Bokus A, Daujat-Chavanieu M, Jorgensen C, Hugnot J, MitoCeption V. Transferring isolated human MSC mitochondria to glioblastoma stem cells. The Journal of Visualized Experiments. 2017; (120):55245. DOI: 10.3791/55245.

41. Andrzejewska A, Dabrowska S, Lukomska B, Janowski M. Mesenchymal stem cells for neurological disorders. Journal of Advanced Research. 2021; 8:2002944. DOI: 10.1002/advs.202002944.

42. Perriot S, Mathias A, Perriard G, Canales M, Jonkmans N, Merienne N, Laplaud D. Human induced pluripotent stem cell-derived astrocytes are differentially activated by multiple sclerosis-associated cytokines. Stem Cell Reports. 2018; 11(5):1199-1210. DOI: 10.1016/j.stemcr.2018.09.015.

43. El-Ghaiesh S, Bahr H, Ibrahiem A, Ghorab D, Alomar S, Farag N, Zaitone S. Metformin protects from rotenone–induced nigrostriatal neuronal death in adult mice by activating AMPK-FOXO3 signaling and mitigation of angiogenesis. Frontiers in Molecular Neuroscience. 2020; 13:84. DOI: 10.3389/fnmol.2020.00084.

44. Watanabe Y, Taguchi K, Tanaka M. Ubiquitin, Autophagy and Neurodegenerative Diseases. Cells. 2020; 9(9):2022. DOI: 10.3390/cells9092022.

45. Mashahreh B, Reiss Y, Wiener R, Ravid T. Methods in Enzymology. Chapter Four-Assays for dissecting the in *vitro* enzymatic activity of yeast Ubc7. Academic Press. 2019; 619:71-95. DOI: 10.1016/bs.mie.2018.12.035.

الملخص العربى

الدور المحتمل للخلايا الجذعية الوسيطة للنخاع العظمي (BM-MSCs) في تحسين التغييرات المستحدثة بواسطة الروتينون على المادة السوداء في ذكر الجرذ الأبيض البالغ: دراسة مورفومترية ونسيجية وهستوكيميائية مناعية

محمد نبيل محمود أحمد، درية عبد الله محمد زغلول، إسراء خالد محمد نفادي، رينيه رفعت بشرى تادرس

قسم التشريح الآدمي وعلم الأجنة ـ كلية الطب ـ جامعة أسيوط

خلفية: يؤدي الفقد للخلايا العصبية الدوبامينية في المادة السوداء إلى حدوث مرض باركنسون. يستخدم الروتينون كنموذج حيواني لاحداث مرض باركنسون. تعتبر الخلايا الجذعية الوسيطة للنخاع العظمي علاجًا واعدًا.

الهدف من الدراسة: تقييم تأثيرات الروتينون على المادة السوداء ودور الخلايا الجذعية الوسيطة لنخاع العظم في تحسين هذه التأثيرات.

المواد وطرق البحث: تم تقسيم إجمالي عدد ٢٤ جرذا بشكل عشوائي إلى ثلاث مجموعات. تم تقسيم المجموعة A إلى: المجموعة A١ (٦ جرذان) تلقت حقنة تحت الجلد بمقدار ٥ مل DMSO / كجم مرة كل يومين لمدة أسبوعين، بينما تلقت المجموعة A٢ (٦ جرذان) نفس النظام لمدة خمسة أسابيع. تلقت المجموعة B (المجموعة المعالجة بالروتينون) (٦ جرذان) حقنة تحت الجلد بجرعة ١,٥ مجم / كجم من الروتينون المذاب في ٥ مل DMSO / كجم، مرة كل يومين لمدة أسبوعين. تم حقن المجموعة C (المجموعة المعالجة بـالخلايا الجذعية الوسيطة لنخاع العظم) (٦ جرذان) بالروتينون بنفس النظام مثل المجموعة B، متبوعًا بحقن واحد مليون من الخلايا الجذعية الوسيطة لنخاع العظم الغير متجانسة مخففة بـ ١ مل محلول ملحي داخل الصفاق و تمت التضحية بها بعد ٣ أسابيع. في الوقت المحدد، تم تخدير الجرذان والتضحية بها، وتمت معالجة الأدمغة من أجل الفحص المجهري الضوئي والإلكتروني و الهستوكيمياء المناعية.

النتائج: تم الكشف عن انخفاض في وزن جسم الجرذان وزيادة في وزن دماغ المجموعة B ذات دلالة إحصائية مقارنةً بالمجموعة الضابطة A١ وكذلك أظهرت المجموعة B علامات تنكس الخلايا العصبية وأجسام ليوي وبنية تحتية عصبية مدمرة. كما أظهرت الدراسة الهستوكيميائية المناعية بواسطة GFAP و caspase-٣وubiquitin ايجابية قوية في نشاط المناعة وتراكم البروتين. أظهرت المجموعة C تحسنًا مورفومتريًا ونسيجيًا وهستوكيميائيا مناعيًا ملحوظًا.

الاستنتاج: يؤثر الروتينون سلبًا على المادة السوداء ويمكن للخلايا الجذعية الوسيطة لنخاع العظم أن تحسن من هذه التأثيرات.